Geophysical Research Letters

RESEARCH LETTER
10.1029/2018GL078864

Jupiter Lightning-Induced Whistler and Sferic Events With Waves and MWR During Juno Perijoves

Masafumi Imai[1], Ondřej Santolík[2,3], Shannon T. Brown[4], Ivana Kolmašová[2,3], William S. Kurth[1], Michael A. Janssen[4], George B. Hospodarsky[1], Donald A. Gurnett[1], Scott J. Bolton[5], and Steven M. Levin[4]

[1]Department of Physics and Astronomy, University of Iowa, Iowa City, IA, USA, [2]Department of Space Physics, Institute of Atmospheric Physics, The Czech Academy of Sciences, Prague, Czechia, [3]Faculty of Mathematics and Physics, Charles University, Prague, Czechia, [4]Jet Propulsion Laboratory, California Institute of Technology, Pasadena, CA, USA, [5]Space Science Department, Southwest Research Institute, San Antonio, TX, USA

Key Points:
- First multi-instrument investigation for Jupiter whistler and sferic events was carried out using Juno
- Whistler and sferic observations were compared on timescales of the order of a few milliseconds
- A new constraint on the whistler-sferic coupling distances was estimated

Correspondence to:
M. Imai,
masafumi-imai@uiowa.edu

Citation:
Imai, M., Santolik, O., Brown, S. T., Kolmašová, I., Kurth, W. S., Janssen, M. A., et al. (2018). Jupiter lightning-induced whistler and sferic events with waves and MWR during Juno perijoves. *Geophysical Research Letters*, *45*, 7268–7276. https://doi.org/10.1029/2018GL078864

Received 23 MAY 2018
Accepted 7 JUL 2018
Accepted article online 13 JUL 2018
Published online 3 AUG 2018

Abstract During the Juno perijove explorations from 27 August 2016 through 1 September 2017, strong electromagnetic impulses induced by Jupiter lightning were detected by the Microwave Radiometer (MWR) instrument in the form of 600-MHz sferics and recorded by the Waves instrument in the form of Jovian low-dispersion whistlers discovered in waveform snapshots below 20 kHz. We found 71 overlapping events including sferics, while Waves waveforms were available. Eleven of these also included whistler detections by Waves. By measuring the separation distances between the MWR boresight and the whistler exit point, we estimated the distance whistlers propagate below the ionosphere before exiting to the magnetosphere, called the coupling distance, to be typically one to several thousand of kilometers with a possibility of no subionospheric propagation, which gives a new constraint on the atmospheric whistler propagation.

Plain Language Summary Lightning at Jupiter produces a strong electromagnetic impulse, which can escape the Jovian atmosphere and enter the inner magnetosphere. Among the lightning, microwave-frequency sferics come from lightning spots, and audio-frequency whistlers propagate away from the spots below the ionosphere. If certain plasma conditions are met, these whistlers can leak into the magnetosphere. Estimates of whistler propagation distances at the planet have not been previously performed. Since the arrival at Jupiter on 5 July 2016, the Juno spacecraft has provided the opportunity to monitor the two kinds of lightning activity with two onboard instruments during its closest approach to Jupiter. This opportunity happens every 53.6 day in the eccentric, polar orbit of Juno. Using data collected during Juno's closest approaches to Jupiter, the whistler propagation distance was estimated to be approximately one to several thousand kilometers, which may be comparable to the terrestrial equivalent. This new approach provides the benefit of understanding multidimensional structures of lightning at Jupiter.

1. Introduction

The discovery of Jupiter's lightning was made independently by the Voyager 1 plasma wave instrument recording Jovian low-frequency whistler waves (Gurnett et al., 1979) and images of Jovian optical flashes (Cook et al., 1979). The whistlers had a dispersion curve on the timescale of seconds in a time-frequency power spectrogram, due to propagation through the high-density magnetized plasma in the Io plasma torus. By virtue of the association between lightning and whistlers at Earth (Helliwell, 1965), the detection of the Jovian whistlers proved the existence of lightning at the planet (Gurnett et al., 1979). Jupiter's whistlers were observed in a frequency range of a few tens of hertz to 7 kHz (Kurth et al., 1985), having the restriction of propagations below either the local electron cyclotron frequency f_{ce} or the local electron plasma frequency f_{pe}, whichever is lower (Stix, 1992). Clouds illuminated from below by lightning were visible in optical wavelengths from Voyager 1 (Cook et al., 1979), Voyager 2 (Borucki & Magalhães, 1992), Galileo (Little et al., 1999), Cassini (Dyudina et al., 2004), and New Horizons (Baines et al., 2007). However, none of the Jovian lightning observations were carried out simultaneously by two or more instruments onboard a spacecraft.

The non-dispersed spectral feature related to lightning at radio wavelengths was first observed at Jupiter by the Galileo Probe in a magnetic field waveform in the frequency range of 10 Hz to 100 kHz (Rinnert et al., 1998). This signal was interpreted as originating from a distant thunderstorm about 15,000 km from the probe (Rinnert & Lanzerotti, 1998). Lightning-induced radio pulses at frequencies above 100 kHz were conjectured, but no detections of this kind were reported in the Jovian inner magnetosphere by Zarka (1985), who inspected the electric field spectra from 20 kHz to 41 MHz from the Voyager planetary radio astronomy instrument (Warwick et al., 1977). He suggested that the Jovian ionosphere prevents these radio pulses from escaping due to strong radio absorption. In order to reconcile the abundance of whistlers and no high-frequency radio pulses, Farrell et al. (1999) proposed a *slow* discharge model in which a radio discharge lasting 1–2 ms is strongly attenuated in the ionosphere at high frequencies but is able to escape into the magnetosphere at low frequency via coupling to the whistler mode.

Another opportunity to examine the nature of Jupiter lightning is provided by the Juno polar-orbiting spacecraft that arrived at Jupiter on 5 July 2016. Since then, Juno has maintained a 53-day eccentric polar orbit around Jupiter, collecting data during seven perijove passes from PJ1 on 27 August 2016 through PJ8 on 1 September 2017 (Bolton et al., 2017). No scientific data were obtained at PJ2 on 19 October 2016. The perijove lightning observations were made at the radial distances between 1.05 R_J and 5 R_J, where R_J = 71,492 km. During these perijove passes, the Juno Microwave Radiometer (MWR) instrument originally recorded 377 lightning radio pulses called *sferics* in a narrowband channel at 600 MHz within 100-ms integration intervals (Brown et al., 2018). More recently, the compiled catalogue was updated to a total of 383 sferic detections. The radio and plasma wave (Waves) instrument has recorded 1,627 Jovian low-dispersion whistlers on the timescale of one to tens of milliseconds and at frequencies below 20 kHz, revealing that Jupiter's lightning flashes are more frequent than previously detected, with lightning rates similar to Earth (Kolmašová et al., 2018). Jovian rapid whistlers, a term used by Kolmašová et al. (2018), are referred to as Jovian low-dispersion whistlers throughout this paper.

In this paper, using two independent catalogues of Jovian low-dispersion whistlers and sferics observed by Juno, we report the details of concurrent whistler and sferic events and deduce the distances that whistlers may propagate below the Jovian ionosphere before exiting to the magnetosphere.

2. Observations

The Waves (Kurth et al., 2017) and MWR (Janssen et al., 2017) instruments are two of nine instruments onboard Juno (Bolton et al., 2017) that operate independently. By chance, these instruments sometimes performed coincident observations that use the spacecraft internal clock to ensure a relative timing accuracy of 10 ms. The spacecraft internal clock is converted to spacecraft event time using Juno SPICE kernels provided by National Aeronautics and Space Administration's Navigation and Ancillary Information Facility (Acton, 1996). Here we use JNO_SCLKSCET.00069.tsc to convert the timing of Waves and MWR data into a common spacecraft event time.

The Waves instrument (Kurth et al., 2017) consists of three receivers, one electric dipole antenna perpendicular to the spin z axis of the spacecraft, and one magnetic search coil sensor parallel to the z axis. By means of one Low Frequency Receiver and two redundant High Frequency Receivers, five different frequency bands are used to measure the electric fields of waves from 50 Hz to 41 MHz with the electric dipole antenna and the magnetic fields of waves from 50 Hz to 20 kHz with the magnetic search coil sensor. The initial survey of Jovian low-dispersion whistlers was done by Kolmašová et al. (2018) using the burst mode of the Low Frequency Receiver electric and magnetic field components from 50 Hz to 20 kHz in 122.88-ms waveform snapshots (comprising 6,144 measurements each). Such snapshots are typically acquired once per second. For the purpose of the present study, the waveforms are converted from the time domain to the spectral domain through 256-point fast Fourier transforms sliding by 32 points for each giving an overlap factor of 7/8, temporal resolution of 640 μs, and spectral resolution of 0.2 kHz.

The MWR instrument (Janssen et al., 2017) comprises six different receivers each with a dedicated, tuned antenna to sample one linearly polarized intensity that is converting into antenna temperature T_A in K for six independent frequency channels at 600 MHz, 1.25 GHz, 2.6 GHz, 5.2 GHz, 10.0 GHz, and 22.0 GHz. Here we refer to normalized antenna temperature $\hat{T}_A$ at 10^4 km as $T_A(h/10^4)^2$, where h is Juno's altitude in kilometer. All antennas are placed perpendicular to the z axis. The temporal resolution of each channel is fixed at 100 ms (99-ms integration time). The antennas rotate 1.2° during each integration interval due to Juno's 30-s rotation

period. The Jovian sferics were reported by Brown et al. (2018) utilizing the 600-MHz channel with a bandwidth of 15 MHz. The 600-MHz patch-array antenna has a 17° half-angle beam at −10 dB covering about 90% of the received power. Therefore, the MWR boresight pinpoints the lightning source within the beam projected onto the 5-bar surface. The detailed description of the determination of the MWR sferic events can be found in Brown et al. (2018).

3. Jovian Whistler and Sferic Analysis

As a result of the comparison of the Waves catalogue of 1,627 Jovian low-dispersion whistlers within 1,311 waveform snapshots (Kolmašová et al., 2018) and the MWR sferic catalogue of 383 lightning events (Brown et al., 2018), we found 11 MWR sferic 100-ms events that overlap with eight Waves 122.88-ms snapshots in which we detected low-dispersion whistlers, hereafter called concurrent events at altitudes between 6,340 and 22,050 km. In addition, we use the term non-concurrent event when the MWR sferic event occurs without any detection of whistlers in the Waves waveforms. We found 60 non-concurrent events at altitudes between 3,510 and 62,060 km. Note that non-concurrent events with low-dispersion whistlers but no sferics cannot be used in this paper, because this shows only an edge of the concentric whistler exit circle from lightning, whose radial distance is unknown. Hence, we cannot measure distances between the lightning source locations and whistler exit points. It is important to note that the inclination of the lightning channel influences the propagation of the emitted waves (Pérez-Invernón, Lehtinen, et al.,2017; Pérez-Invernón, Luque, et al., 2017). Although this inclination may influence the relative intensities of MWR and Waves received signals, a small number of only eleven concurrent events in this study does not allow us to investigate this influence.

Figure 1 shows a summary of all of the concurrent events. In order to account for the dispersion curves of whistlers, we have performed a group delay computation using the Juno Reference Model through Perijove 9 (JRM09) internal magnetic field model with spherical harmonic coefficients of 10 (Connerney et al., 2018), which defines the electron cyclotron frequency as a function of position along the field line passing through Juno. The modeled magnetic field strength was rescaled to the actual locally measured one within 3% from the model values. However, the 3% difference results from the fact that the use of the degree 10 approximation neglects terms of higher degree determined by the JRM09 model fit. We also use ionospheric plasma density models based on entry and exit radio occultation measurements of Voyager 2 (Hinson et al., 1998), which define the plasma frequency as a function of altitude. These models have been used as an input for the group delay computation based on the cold plasma approximation and described in detail by Kolmašová et al. (2018). We found that the whistlers were reasonably reproduced by the modeled group delays (depicted by dotted gray lines) using the Voyager 2 entry ionospheric profile for Figures 1a and 1b, but for all the other cases, a decreased density to 30% of its model value had to be used in order to fit the observed dispersion (Figures 1c–1h). We repeated our whistler dispersion computations using the Voyager 2 exit ionospheric model (not shown here) instead of the entry model. The resulting differences of the whistler dispersion shapes were very small and negligible, but it is necessary to reduce to 30% of the plasma density for the cases of Figures 1a and 1b and to 10% for the other cases. A similar need for lower densities than the model values has also been noted by Kolmašová et al. (2018). It is interesting to note that this decrease of plasma densities in the lower ionosphere could favor the inception of Jovian transient luminous events triggered by lightning (Luque et al., 2014; Pérez-Invernón, Luque, et al., 2017; Yair et al., 2009).

Whistlers can be classified as to whether they propagate along a magnetic field line or not (Smith & Angerami, 1968). Field-aligned propagating whistlers are called *ducted* whistlers (Helliwell, 1965). Hence, the magnetic footprint can be estimated by mapping along the modeled JRM09 magnetic field line (Connerney et al., 2018) from Juno onto the Jovian atmosphere at an altitude of 300 km above the 1-bar level. Using this method, we locate the Waves whistler footprints as the orange plus marks for the concurrent events and as the white plus marks for the noncurrent events in Figure 2a. Likewise, we assign the MWR sferic boresights as yellow stars for the concurrent events and as white stars for the non-concurrent events. It is clear that the non-concurrent events are found at almost all latitudes but with a preference for northern latitudes between 30° and 80°. In contrast, the concurrent events are concentrated in three regions in Figures 2b–2d. The yellow ellipses indicate the 17° half-angle beam at −10 dB projected onto the 5-bar surface as source level for Jovian lightning (e.g., Dyudina et al., 2004) centered on the MWR boresights. Most pairs are contained inside of these yellow ellipses in Figures 2b–2d. This means that the lightning-induced impulses may escape without any subionospheric propagation, just vertically above the lightning location and form both detected sferics and low-dispersion whistlers. However, these impulses might also propagate for some limited distance below

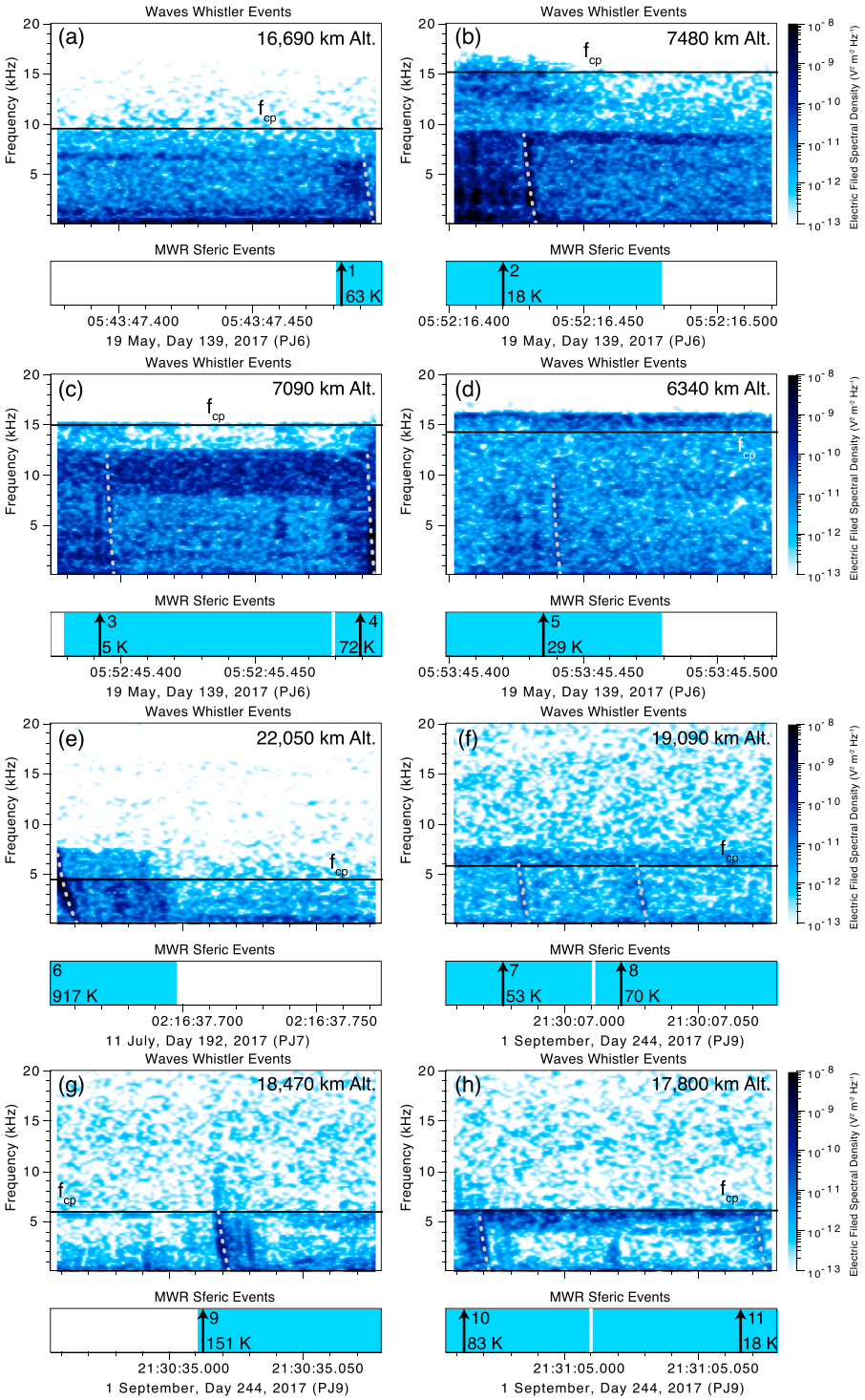

Figure 1. Concurrent whistler and sferic events using data set of whistler detections by Waves (Kolmašová et al., 2018) and sferic detections by Microwave Radiometer (MWR) (Brown et al., 2018). The borders of the blue bars indicate the beginning and end time of MWR sferic events (100-ms integration intervals), which overlap the times of Waves whistler detections. The black lines are the local proton cyclotron frequency, f_{cp}, computed from Juno's onboard magnetometer (Connerney et al., 2017). The gray dotted lines are consequences of the group delay computations. The Voyager 2 ionospheric profile at radio occultation entry (Hinson et al., 1998) is used for (a) and (b), and the same profile with 30% decreased densities is utilized for (c–h). Intensity of each MWR sferic in normalized antenna temperature $\hat{T}_A$ at 10^4 km is shown near an arrow that gives the light arrival time of the sferic, relative to the corresponding whistler trace in all figures but (e). For (e), the estimated light arrival time was 2:16:37.646 on 11 July 2017, which is outside of the figure but within the MWR sferic event. The events are labeled the numerals of 1 to 11 next to the arrows.

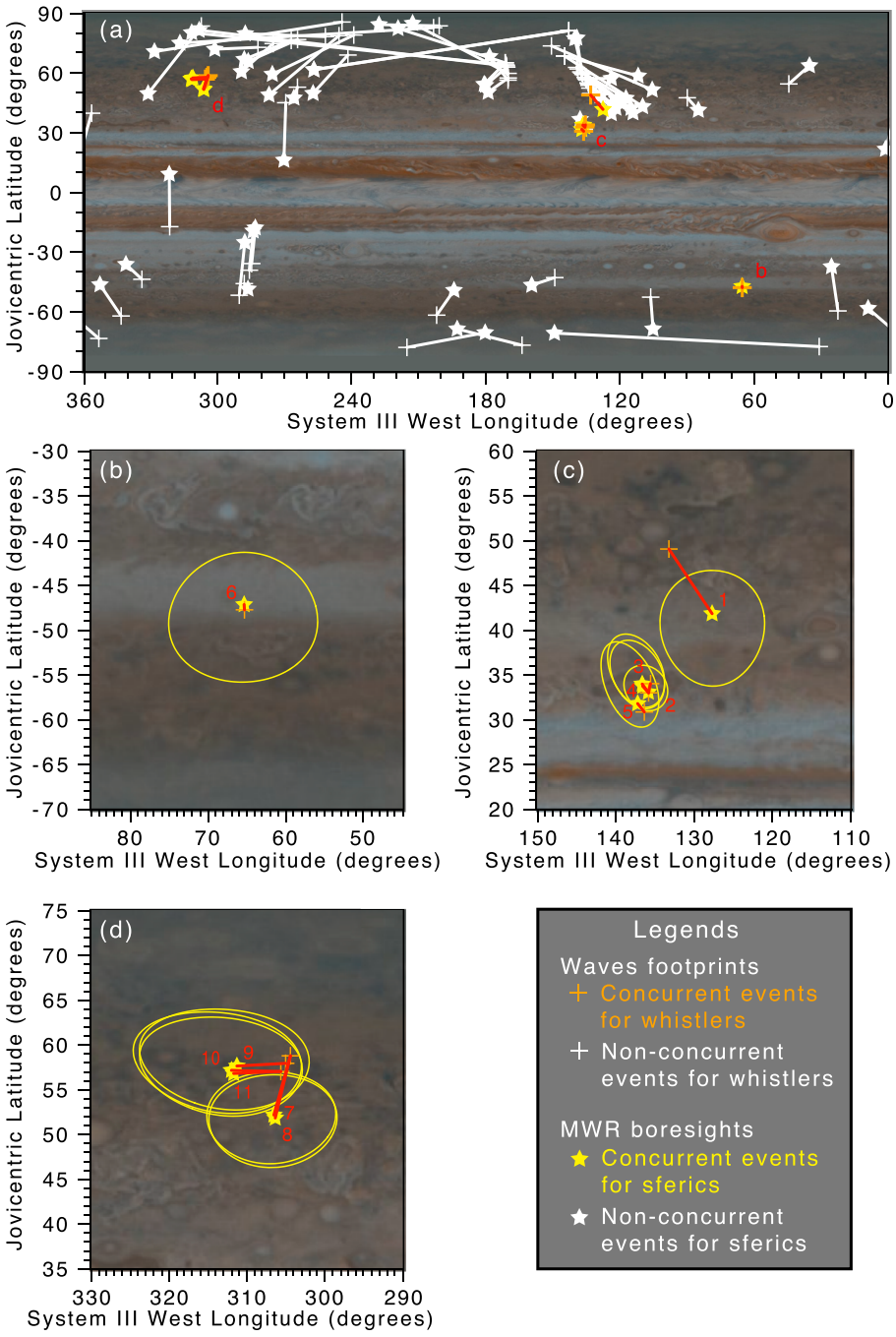

Figure 2. (a) Global distribution map of the concurrent and non-concurrent whistler and sferic events. The non-concurrent events are those observations of sferics by MWR with no corresponding whistlers observed by Waves. The detailed regions are shown for time spans of (b) 02:16:38 on 11 July 2017, (c) 05:43:47–05:53:46 on 19 May 2017, and (d) 21:30:07–21:31:05 on 1 September 2017. The numerals correspond to the concurrent events in Figure 1. The yellow ellipses indicate the MWR beam projections for 17° half-angle at −10 dB (Janssen et al., 2017).

Table 1
Estimated Parameters for Three Groups from Concurrent Events

Groups	Number of events in Figure 1	$\hat{T}_A$ (K) Range	Wf-Mb separation distance[a](km) Mean	Uncertainty[b]
1	5 (2–6)	5–917	1,200	630–10,330
2	3 (9–11)	18–151	3,990	3,880–5,860
3	3 (1, 7, 8)	53–70	8,740	60–6,670

[a]Wf and Mb stand for the Waves magnetic footprints and Microwave Radiometer (MWR) boresights, respectively. [b]The uncertainty is a deviation of the distance to the MWR boresight from the upper and lower bounds. These boundaries are the distances to the near and far edges of the MWR 17° beam ellipse, respectively.

the Jovian ionosphere before escaping to the ionosphere. The maximum propagation distance can be estimated as the distance from the footprint to the far edge of the MWR uncertainty ellipse.

To further quantify the separation distance between the MWR beam and the whistler exit point, we utilize both concurrent and non-concurrent whistler and sferic events. In this study, five assumptions were made: (1) the Waves low-dispersion whistler and the concurrent MWR sferic originate from the same source lightning stroke localized at the MWR boresight projection at the 5-bar level with an uncertainty defined by the projection of the 17° beam, (2) the Waves low-dispersion whistlers are ducted, (3) their exit points are magnetically mapped from the spacecraft to 300-km altitude, then vertically projected downward onto the 5-bar level, (4) that JRM09 accurately models Jupiter's magnetic field in this region of the magnetosphere, and (5) the separation distance D is approximately written as

$$D = \arccos\left(\frac{\mathbf{W}\cdot\mathbf{M}}{\sqrt{\mathbf{W}\cdot\mathbf{W}}\sqrt{\mathbf{M}\cdot\mathbf{M}}}\right)\frac{\sqrt{\mathbf{W}\cdot\mathbf{W}}+\sqrt{\mathbf{M}\cdot\mathbf{M}}}{2}, \quad (1)$$

where **W** and **M** are the Cartesian coordinates in the Jovicentric System III coordinates for the whistler exit point and MWR boresight, respectively.

As a result, the separation distance between the MWR boresight and whistler exit point is depicted as a function of $\hat{T}_A$ for the concurrent and non-concurrent whistler and sferic events in Figures 3a and 3b, respectively. For the concurrent events, groups 1, 2, and 3 may be categorized on the basis of the mean separation distances of 1,200, 3,990, and 8,740 km. For these groups, the number of events in Figure 1, the MWR $\hat{T}_A$ range, and the estimates of separation distances are summarized in Table 1. The lowest limits of the separation distances range from 7,000 to 10,000 km for group 3 and 0 km (no subionospheric propagation) for groups 1 and 2 in Figure 3a. This implies that, in group 3, the actual locations of lightning generating the whistlers might be different from those of the sferics. The whistlers might originate from a distant lightning thunderstorm (coincidentally occurring at the same or close times) outside of the MWR boresight regions. In contrast, the lightning source locations for pairs of the whistlers and sferics for groups 1 and 2 match each other. This interpretation for group 3 does not hold for our assumption (1). On the other hand, groups 1 and 2 occur at much lower separation distances compared to most of non-concurrent events in Figure 3b, for which the estimates of separation distances start at 3,260 km. In summary, the waves at kilohertz frequencies may propagate below the ionosphere at distances below 10,000 km, more probably below 1,000–4,000 km, but the total absence of subionospheric propagation still cannot be excluded based on our data set.

Another hypothetically possible class of whistlers are known as *unducted* whistlers (Smith & Angerami, 1968) that can propagate at an angle with respect to the planetary magnetic field and for which our assumption (2) does not hold. Since we do not know this angle, we can, in a simple approximation, assume vertical propagation from the source to Juno. In reality, unducted whistlers would be emitted from a point somewhere between this vertical footprint and the previously discussed magnetic footprint. Figures 3c and 3d are the same format as Figures 3a and 3b but for the separation distances between the whistler exit points assuming vertical propagation and the MWR boresight. The results are roughly similar to those in Figures 3a and 3b, showing a possibility of subionospheric propagation and distance below 8,000 km (maximum value of the lowest limits of the separation distances in Figure 3c), not excluding the possibility of the absence of propagation below the ionosphere.

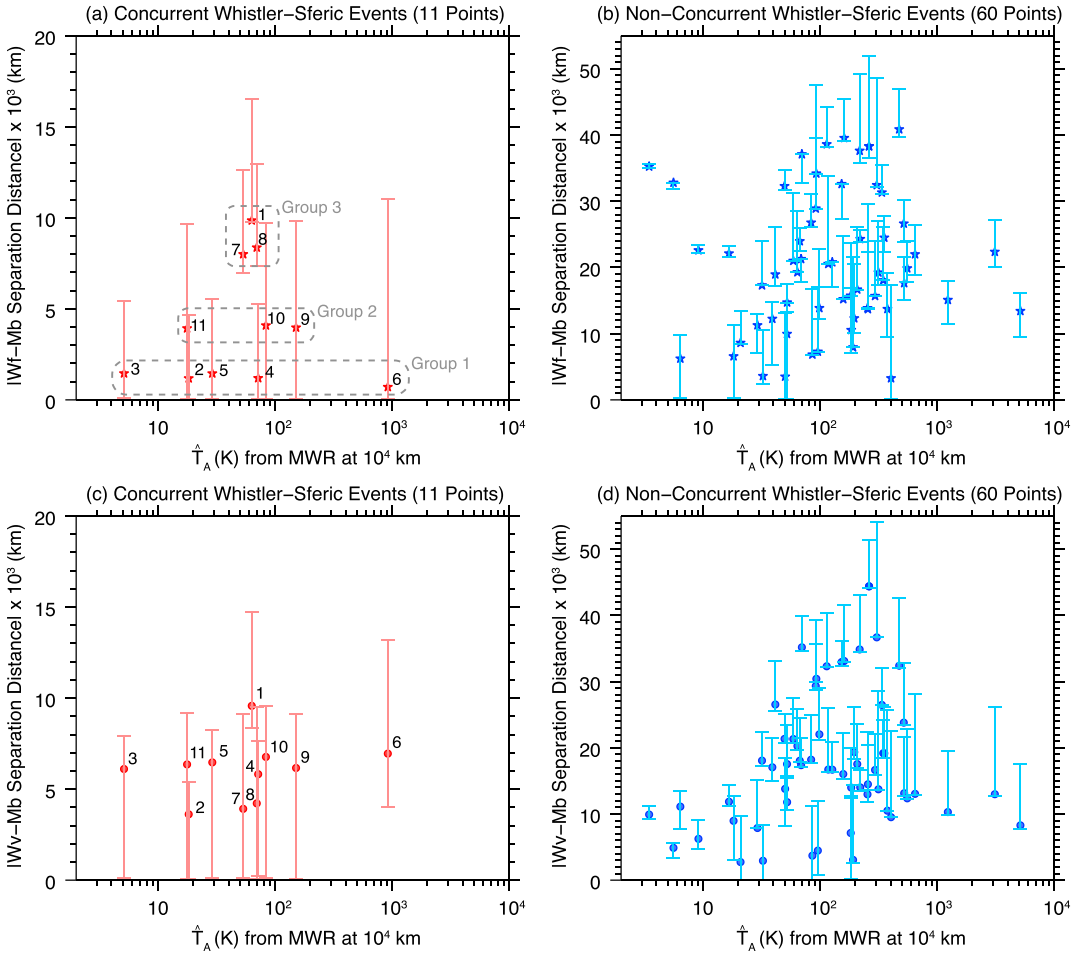

Figure 3. (a, b) Separation distances of pairs of Waves magnetic footprints (Wf) and MWR boresights (Mb) and (c, d) pairs of Waves vertical points (Wv) and Mb plotted as a function of the MWR $\hat{T}_A$ at 10^4 km of Juno's altitude above the 1-bar level. The concurrent events are shown in (a) and (c), and the non-concurrent events are displayed in (b) and (d). The separation distances for the upper and lower bounds of the error bars are computed from the whistler footprint to the nearer edge of the MWR ellipse and the most distant edge of the ellipse, respectively. Additionally, the numerals in (a) and (c) refer to Figure 1.

4. Summary

In this paper, we report the first multi-instrument investigation of Jupiter lightning by examining whistler and sferic events obtained by the Waves and MWR instruments onboard Juno. We compare the Waves catalogue of Jovian low-dispersion whistlers compiled by Kolmašová et al. (2018) and the MWR 600-MHz sferic catalogue produced by Brown et al. (2018) during the course of Juno perijove passes from 27 August 2016 through 1 September 2017. We found 71 overlapping Waves and MWR observations during which a sferic was detected. Eleven of these also included whistler detections (concurrent events) and the remaining 60 had MWR sferic detections without any whistlers in the Waves waveform snapshots (non-concurrent events). We do not investigate the non-concurrent events in which Waves low-dispersion whistlers are detected but with no MWR sferic detections. We assumed that the lightning source location at the 5-bar level is determined by the MWR boresight with a 17° beam width (−10-dB level), and the whistler exit point corresponds to the point mapped along the modeled magnetic field line onto the Jovian atmosphere at 300-km altitude above the 1-bar level. Analyzing the concurrent and non-concurrent events is important to independently determine the lower and upper limits of the separation distance. Therefore, the typical separation distance between two points is 1,000–4,000 km (less than 10,000 km), but a direct exit without the subionospheric propagation cannot be excluded. Analogous to Jovian whistlers, the separation distance between terrestrial whistlers and their respective lightning strokes was experimentally found to be 2,000 km using ground stations

(Storey, 1953) and up to 1,000–10,000 km using both ground and spaceborne instruments (Burkholder et al., 2013; Fiser et al., 2010; Santolík et al., 2009). Therefore, the Jovian separation distance might be comparable to the terrestrial one.

The separation distance between a lightning source and the whistler exit point represents the distance along which the electromagnetic waves in the several kilohertz range can couple into the whistler mode and thereby exit through the ionosphere. This is referred to as the coupling distance in this paper. The coupling distance is important as an estimate of the area represented by a whistler detection, hence can be used to estimate the areal lightning flash rate in flashes per year kilometer squared. According to ray-tracing computations (Rinnert et al., 1979), Scarf et al. (1981) determined the area to be 10^6 km^2, which is comparable to or one order of magnitude smaller than our estimates. Kolmašová et al. (2018) analyzed the global distribution of low-dispersion whistlers detected by Juno, finding that they occur more frequently in the midlatitude region with an average rate of 1 whistler/s. Assuming an area of 10^6 to 10^7 km^2, the lightning flash rate is 3–30 flashes/year/km^2 (Kolmašová et al., 2018) for the midlatitude region at Jupiter, which is comparable to a global average rate of 2.7 flashes/year/km^2 at Earth (Christian et al., 2003).

There are over two thousand total detections of low-dispersion whistlers and 600-MHz sferics, the largest data set of Jovian lightning thus far. And, with Juno continuing its mission, the data set will grow. The simultaneous detection of lightning with whistlers and sferics solidifies the connection of both of these phenomena with lightning strokes and will lead to a better understanding of Jovian lightning and the propagation of these emissions in the Jovian environment.

Acknowledgments
The authors are pleased to acknowledge all members of the Juno mission team, especially the engineers and staff of the Juno Waves and MWR instruments. They thank J. E. P. Connerney for his kind assistance in providing the Juno magnetometer data and clarifying the description of JRM09 model. They are also grateful to the reviewers for fruitful comments and their careful reading of the manuscript. The research at the University of Iowa was supported by NASA through Contract 699041X with the Southwest Research Institute. The work of I. K. and O. S. was supported by the MSM100421701 and LTAUSA17070 grants and by the Praemium Academiae award. M. I. appreciates the Institute of Atmospheric Physics of the Czech Academy of Sciences for the kind hospitality during his 3-week visit in October 2017. The Juno SPICE kernels are available via the NASA NAIF website (https://naif.jpl.nasa.gov/pub/naif/JUNO/kernels/). The Juno data used in this study are publicly accessible through the Planetary Data System (https://pds.nasa.gov).

References

Acton, C. H. Jr. (1996). Ancillary data services of NASA's navigation and ancillary information facility. *Planetary and Space Science*, *44*(1), 65–70. https://doi.org/10.1016/0032-0633(95)00107-7

Baines, K. H., Simon-Miller, A. A., Orton, G. S., Weaver, H. A., Lunsford, A., Momary, T. W., et al. (2007). Polar lightning and decadal-scale cloud variability on Jupiter. *Science*, *318*(5848), 226–229. https://doi.org/10.1126/science.1147912

Bolton, S. J., Lunine, J., Stevenson, D., Connerney, J. E. P., Levin, S., Owen, T. C., et al. (2017). The Juno mission. *Space Science Reviews*, *213*(1–4), 5–37. https://doi.org/10.1007/s11214-017-0429-6

Borucki, W. J., & Magalhães, J. A. (1992). Analysis of Voyager 2 images of Jovian lightning. *Icarus*, *96*(1), 1–14. https://doi.org/10.1016/0019-1035(92)90002-O

Brown, S., Janssen, M., Adumitroaie, V., Atreya, S., Bolton, S., Gulkis, S., et al. (2018). Prevalent lightning sferics at 600 megahertz near Jupiter's poles. *Nature*, *558*, 87–90. https://doi.org/10.1038/s41586-018-0156-5

Burkholder, B. S., Hutchins, M. L., McCarthy, M. P., Pfaff, R. F., & Holzworth, R. H. (2013). Attenuation of lightning-produced sferics in the Earth-ionosphere waveguide and low-latitude ionosphere. *Journal of Geophysical Research: Space Physics*, *118*, 3692–3699. https://doi.org/10.1002/jgra.50351

Christian, H. J., Blakeslee, R. J., Boccippio, D. J., Boeck, W. L., Buechler, D. E., Driscoll, K. T., et al. (2003). Global frequency and distribution of lightning as observed from space by the optical transient detector. *Journal of Geophysical Research*, *108*(D1), 4005. https://doi.org/10.1029/2002JD002347

Connerney, J. E. P., Benn, M., Bjarno, J. B., Denver, T., Espley, J., Jorgensen, J. L., et al. (2017). The Juno magnetic field investigation. *Space Science Reviews*, *213*(1–4), 39–138. https://doi.org/10.1007/s11214-017-0334-z

Connerney, J. E. P., Kotsiaros, S., Oliversen, R. J., Espley, J. R., Joergensen, J. L., Joergensen, P. S., et al. (2018). A new model of Jupiter's magnetic field from Juno's first nine orbits. *Geophysical Research Letters*, *45*, 2590–2596. https://doi.org/10.1002/2018GL077312

Cook, A. F., Duxbury, T. C., & Hunt, G. E. (1979). First results on Jovian lightning. *Nature*, *280*, 794. https://doi.org/10.1038/280794a0

Dyudina, U. A, Del Genio, A. D, Ingersoll, A. P., Porco, C. C., West, R. A., Vasavada, A. R., et al. (2004). Lightning on jupiter observed in the H_α line by the Cassini Imaging Science Subsystem. *Icarus*, *172*(1), 24–36. https://doi.org/10.1016/j.icarus.2004.07.014

Farrell, W. M., Kaiser, M. L., & Desch, M. D. (1999). A model of the lightning discharge at Jupiter. *Geophysical Research Letters*, *26*(16), 2601–2604. https://doi.org/10.1029/1999GL900527

Fiser, J., Chum, J., Diendorfer, G., Parrot, M., & Santolik, O. (2010). Whistler intensities above thunderstorms. *Annales de Geophysique*, *28*(1), 37–46. https://doi.org/10.5194/angeo-28-37-2010

Gurnett, D. A., Shaw, R. R., Anderson, R. R., Kurth, W. S., & Scarf, F. L. (1979). Whistlers observed by Voyager 1: Detection of lightning on Jupiter. *Geophysical Research Letters*, *6*(6), 511–514. https://doi.org/10.1029/GL006i006p00511

Helliwell, R. A. (1965). *Whistlers and related ionospheric phenomena*. Stanford, California: Stanford University Press.

Hinson, D. P., Twicken, J. D., & Karayel, E. T. (1998). Jupiter's ionosphere: New results from Voyager 2 radio occultation measurements. *Journal of Geophysical Research*, *103*(A5), 9505–9520. https://doi.org/10.1029/97JA03689

Janssen, M. A., Oswald, J. E., Brown, S. T., Gulkis, S., Levin, S. M., Bolton, S. J., et al. (2017). MWR: Microwave radiometer for the Juno mission to Jupiter. *Space Science Reviews*, *213*(1–4), 139–185. https://doi.org/10.1007/s11214-017-0349-5

Kolmašová, I., Imai, M., Santolík, O., Kurth, W. S., Hospodarsky, G. B., Gurnett, D. A., et al. (2018). Discovery of rapid whistlers close to Jupiter implying similar lightning rates to those on Earth. *Nature Astronomy*, *2*, 544–548. https://doi.org/10.1038/s41550-018-0442-z

Kurth, W. S., Hospodarsky, G. B., Kirchner, D. L., Mokrzycki, B. T., Averkamp, T. F., Robison, W. T., et al. (2017). The Juno Waves investigation. *Space Science Reviews*, *213*(1–4), 347–392. https://doi.org/10.1007/s11214-017-0396-y

Kurth, W. S., Strayer, B. D., Gurnett, D. A., & Scarf, F. L. (1985). A summary of whistlers observed by Voyager 1 at Jupiter. *Icarus*, *61*(3), 497–507. https://doi.org/10.1016/0019-1035(85)90138-1

Little, B., Anger, C. D., Ingersoll, A. P., Vasavada, A. R., Senske, D. A., Breneman, H., et al. (1999). Galileo images of lightning on Jupiter. *Icarus*, *142*(2), 306–323. https://doi.org/10.1006/icar.1999.6195

Luque, A., Dubrovin, D., Gordillo-Vázquez, F. J., Ebert, U., Parra-Rojas, F. C., Yair, Y., & Price, C. (2014). Coupling between atmospheric layers in gaseous giant planets due to lightning-generated electromagnetic pulses. *Journal of Geophysical Research: Space Physics*, *119*, 8705–8720. https://doi.org/10.1002/2014JA020457

Pérez-Invernón, F. J., Lehtinen, N. G., Gordillo-Vázquez, F. J., & Luque, A. (2017). Whistler wave propagation through the ionosphere of Venus. *Journal of Geophysical Research: Space Physics*, *122*, 11633–11644. https://doi.org/10.1002/2017JA024504

Pérez-Invernón, F. J., Luque, A., & Gordillo-Vázquez, F. J. (2017). Three-dimensional modeling of lightning-induced electromagnetic pulses on Venus, Jupiter, and Saturn. *Journal of Geophysical Research: Space Physics*, *122*, 7636–7653. https://doi.org/10.1002/2017JA023989

Rinnert, K., & Lanzerotti, L. J. (1998). Radio wave propagation below the Jovian ionosphere. *Journal of Geophysical Research*, *103*(E10), 22993–22999. https://doi.org/10.1029/98JE01968

Rinnert, K., Lanzerotti, L., Krider, E., Uman, M., Dehmel, G., Gliem, F., & Axford, W. (1979). Electromagnetic noise and radio wave propagation below 100 kHz in the Jovian atmosphere 1. The equatorial region. *Journal of Geophysical Research*, *84*(A9), 5181–5188. https://doi.org/10.1029/JA084iA09p05181

Rinnert, K., Lanzerotti, L. J., Uman, M. A., Dehmel, G., Gliem, F. O., Krider, E. P., & Bach, J. (1998). Measurements of radio frequency signals from lightning in Jupiter's atmosphere. *Journal of Geophysical Research*, *103*(E10), 22,979–22,992. https://doi.org/10.1029/98JE00830

Santolík, O., Parrot, M., Inan, U. S., Burešová, D., Gurnett, D. A., & Chum, J. (2009). Propagation of unducted whistlers from their source lightning: A case study. *Journal of Geophysical Research*, *114*, A03212. https://doi.org/10.1029/2008JA013776

Scarf, F. L., Gurnett, D. A., Kurth, W. S., Anderson, R. R., & Shaw, R. R. (1981). An upper bound to the lightning flash rate in Jupiter's atmosphere. *Science*, *213*(4508), 684–685. https://doi.org/10.1126/science.213.4508.684-a

Smith, R. L., & Angerami, J. J. (1968). Magnetospheric properties deduced from OGO 1 observations of ducted and nonducted whistlers. *Journal of Geophysical Research*, *73*(1), 1–20. https://doi.org/10.1029/JA073i001p00001

Stix, T. H. (1992). *Waves in plasmas*. New York: Springer-Verlag.

Storey, L. R. O. (1953). An investigation of whistling atmospherics. *Philosophical Transactions of the Royal Society of London, Series A*, *246*(908), 113–141. https://doi.org/10.1098/rsta.1953.0011

Warwick, J. W., Pearce, J. B., Peltzer, R. G., & Riddle, A. C. (1977). Planetary radio astronomy experiment for Voyager missions. *Space Science Reviews*, *21*(3), 309–327. https://doi.org/10.1007/BF00211544

Yair, Y., Takahashi, Y., Yaniv, R., Ebert, U., & Goto, Y. (2009). A study of the possibility of sprites in the atmospheres of other planets. *Journal of Geophysical Research*, *114*, E09002. https://doi.org/10.1029/2008JE003311

Zarka, P. (1985). On detection of radio bursts associated with Jovian and Saturnian lightning. *Astronomy & Astrophysics*, *146*(1), L15–L18.